Effect of Evolved Interactions in Poly(butylene succinate)/Fumed Silica Biodegradable *In Situ* Prepared Nanocomposites on Molecular Weight, Material Properties, and Biodegradability

Alexandros A. Vassiliou,[1] Dimitrios Bikiaris,[1] Khalil El Mabrouk,[2] Marianna Kontopoulou[3]

[1]*Laboratory of Polymer Chemistry and Technology, Department of Chemistry, Aristotle University of Thessaloniki, GR-541 24 Thessaloniki, Macedonia, Greece*
[2]*Nanofabrication Laboratory Group, Institute of Nanomaterials and Nanotechnology, ENSET, Av. de l'Armée Royale, Madinat El Irfane 10 100, Rabat, Morocco*
[3]*Department of Chemical Engineering, Queen's University, Kingston, Ontario, Canada K7L 3N6*

Received 17 February 2010; accepted 28 May 2010
DOI 10.1002/app.32887
Published online 25 August 2010 in Wiley Online Library (wileyonlinelibrary.com).

ABSTRACT: Poly(butylene succinate) (PBSu)/fumed silica nanocomposites were prepared *in situ* by condensation polymerization. TEM micrographs verified that the dispersion of the nanoparticles was homogeneous in the PBSu matrix, while some small agglomerates were also formed at a higher SiO_2 content. ^{13}C NMR spectra affirmed that the hydroxyl end groups of PBSu could form covalent bonds with the surface silanol groups of SiO_2. These interactions affected the molecular weight of the prepared nanocomposites. At low concentrations the SiO_2 nanoparticles acted as chain extenders, increasing the molecular weight of PBSu, while at higher loadings they resulted in extended branching and crosslinking reactions, leading to gradually decreased molecular weights. Silica nanoparticles acted as nucleating agents, increasing the crystallization rate of PBSu. However, the degree of crystallinity was slightly reduced. Tensile strength and Young's modulus were significantly increased with increasing SiO_2 content. The presence of the nanoparticles resulted in reduced enzymatic hydrolysis rates compared to pure PBSu, attributed to the smaller available organic surface, due to the incorporation of SiO_2, and to the existence of branched and crosslinked macromolecules. Dynamic mechanical and rheological properties were also extensively studied.
 J Appl Polym Sci 119: 2010–2024, 2011

Key words: nanocomposites; aliphatic polyester; poly(butylene succinate); fumed silica; enzymatic hydrolysis

INTRODUCTION

Polyesters play a dominant role in the field of biodegradable plastics, due to their hydrolysable ester bonds. Polyesters are made up of two major groups consisted by linear macromolecules, namely aliphatic, and aromatic polyesters. Biodegradable polyesters which have been developed and used commercially are aliphatic, such as poly(lactic acid) (PLA), polycaprolactone (PCL), poly(hydroxy alkanoates) (PHA), poly(butylene succinate) PBSu, and alipharomatic polyesters, such as poly(butylene adipate terephtalate) (PBAT). While common aromatic polyesters, such as PET and PBT, exhibit excellent material properties, they have proven to be almost totally resistant to microbial attack. Aliphatic polyesters on the other hand are readily biodegradable, but on the downside are much more expensive and lack sufficient mechanical properties critical for most applications. All polyesters degrade eventually, with hydrolysis (degradation induced by water) being the dominant mechanism. Synthetic aliphatic polyesters are usually synthesized from the corresponding diols and dicarboxylic acids via condensation polymerization, and have been shown to be completely biodegradable in soil and water.

Poly(butylene succinate) (PBSu) is a biodegradable aliphatic semicrystalline polyester, possessing very attractive properties. It exhibits a melting point similar to that of low-density polyethylene (LDPE) and its tensile strength lies between that of high density polyethylene (HDPE) and isotactic polypropylene (PP). Furthermore, PBSu has several interesting properties, apart from the aforementioned biodegradability characteristics, such as melt processibility and chemical resistance, which open up a wide area of potential applications.[1–11] However, there are significant shortcomings in other properties of PBSu, such as insufficient stiffness, low-melt strength and viscosity. To overcome

Correspondence to: D. Bikiaris (dbic@chem.auth.gr).

some of these drawbacks PBSu has been copolymerized with adipic acid in the presence of a multifunctional glycol and the produced copolymer was found to be exceptional for production of films or bottles, without significantly altered biodegradation characteristics. This copolymer is commercially available under the trade name Bionolle™, supplied by Showa Polymers, Japan.

In recent years great interest has arisen in the formulation and association of biopolymers with nanosized fillers, which could potentially result in a large range of improved properties and render the materials fully competitive with conventional thermoplastics.[12] Similar efforts to improve some of PBSu's properties, especially mechanical, thermal and gas barrier, flame retardant properties, but the dimensional stability of polymeric materials as well, by the incorporation of nanoparticles in the polymer matrix have been carried out.[13–26] Most articles in the literature have focused on the preparation of PBSu nanocomposites with layered silicates.[13–22] However, SiO_2 and multi-walled carbon nanotubes have also been recently used.[15,23,24] PBSu/clay nanocomposites were successfully prepared through the direct insertion of the PBSu polymer chains from the solution between the clay sheds.[17] Characterization of the prepared nanocomposites by Dynamic Mechanical Analysis (DMA) showed significant improvements in the storage modulus when compared to that of neat PBSu. The rheological properties of PBSu/organically modified layered silicate (OMLS) nanocomposites were studied in detail, because the rheological behavior of polymer/OMLS nanocomposites is strongly influenced by their nanostructure and the interfacial characteristics.[18]

Among the numerous inorganic/organic nanocomposites, polymer/silica composites are among the most commonly reported in the literature.[27] They have recently received much attention and are employed in a variety of applications, becoming a quickly expanding field of research. Among the advantages of this nanoparticle is the ease of synthesis and surface treatment, to enhance the interactions with the matrix.[27–29] Furthermore, fumed silica in particular, which was used in this study, owing to its completely amorphous state is considered thoroughly nontoxic and nonirritating.

The aim of the present work was to prepare PBSu/SiO_2 nanocomposites by the *in situ* polymerization technique and investigate the potential interactions taking place between the hydroxyl end groups of PBSu and the surface silanol groups of SiO_2. Furthermore, the effect of the nanoparticles' concentration and of the evolved interactions with the polymer on its thermal, mechanical, dynamic mechanical, rheological, enzymatic hydrolysis, and gas permeability properties was extensively studied.

EXPERIMENTAL

Materials

Succinic acid (Su) (purum 99+%), 1,4-butanediol (Bu) (Purity > 99.7%) and titanium (IV) butoxide (≥97%), (TBT) were obtained from Aldrich Chemical and used as received. Fumed silica nanoparticles (SiO_2) under the trade name AEROSIL® 200 were supplied by Degussa AG (currently Evonik Industries), (Hanau, Germany). The nanoparticles had an average primary particle size of 12 nm, a specific surface area of 200 $m^2\ g^{-1}$ and a SiO_2 content > 99.8%. All other materials and solvents used in the analytical methods were of analytical grade.

Nanocomposites preparation

Nanocomposites of poly(butylene succinate) (PBSu) were prepared *in situ* by the two-stage melt polycondensation of succinic acid and 1,4-butanediol in a glass batch reactor at a mol ratio of 1 : 1.3 Su : Bu. The polymerization mixture, after being placed in a 250 cm^3 round bottomed flask, was degassed and purged with dry nitrogen three times. Thereupon, the mixture was heated under a nitrogen atmosphere for 3 h at 200°C under constant stirring (350 rpm) and water was removed by distillation as the reaction by-product of esterification. Appropriate amount of nanoparticles were first dispersed in 1,4-butanediol by ultrasonic vibration (50 W, Hielscher UP50H) and intense stirring with a magnetic stirrer (300 rpm) for 10 min prior to polymerization

Afterward, for the second reaction stage of polycondensation, 0.3 wt % of Triphenyl phosphate (TPP) as heat stabilizer and 1.0×10^{-3} mol of TBT per mole of succinic acid were added. Reaction was continued under increased mechanical stirring (720 rpm) and high vacuum (~ 5.0 Pa), which was applied slowly over a period of time of about 30 min, to avoid excessive foaming and to minimize oligomer sublimation, at 220 and 240°C for 1-h interval, respectively. Polymerization was stopped by fast cooling to room temperature.

For the preparation of nanocomposites containing 0.5, 1, 2.5, and 5 wt % fumed silica nanoparticles the aforementioned procedure was used, appropriately adjusting the initial SiO_2 nanoparticles' amount dispersed in the diol.

Gel permeation chromatography (GPC)

GPC analysis was performed using a Waters 150C GPC equipped with a differential refractometer as detector and three ultrastyragel (103, 104, 105 å) columns in series. $CHCl_3$ was used as the eluent (1 mL min^{-1}) and the measurements were performed at 35°C. Calibration was performed using polystyrene

standards with a narrow molecular weight distribution. The samples were filtered prior to the measurements.

Nuclear magnetic resonance (NMR)

^{1}H NMR and ^{13}C NMR spectra of the nanocomposites were obtained using a Bruker spectrometer operating at a frequency of 400 MHz for protons. Deuterated chloroform ($CDCl_3$) was used as solvent to prepare solutions of 5% w/v. The number of scans was 10 and the sweep width was 6 kHz.

Differential scanning calorimeter (DSC)

DSC study was performed on a Setaram DSC141 differential scanning calorimeter. Samples of 6.0 ± 0.2 mg were used for every new measurement. A constant nitrogen flow was maintained to provide a constant thermal blanket within the DSC cell, thus eliminating thermal gradients and ensuring the validity of the applied calibration standard from sample to sample. For each sample a cyclic scanning procedure was followed to record the thermal behavior of the material. The procedure involved: (a) heating up to 150°C at a heating rate of 5.0°C min^{-1} and holding at this temperature for 5 min to erase any thermal history of the sample, (b) rapid cooling to −80°C and equilibration, (c) reheating at a heating rate of 5.0°C min^{-1} up to 150°C and holding for 5 min (d) final cooling at a cooling rate of 5°C min^{-1} down to −80°C.

Transmission electron microscopy

Electron diffraction (ED) and transmission electron microscopy (TEM) observations were made on ultra thin film samples of the various nanocomposites prepared by an ultra-microtome. These thin films were deposited on copper grids. ED patterns and TEM micrographs were obtained using a JEOL 120 CX microscope operating at 120 kV. To avoid the destruction of the films after exposure to the electron irradiation, an adequate sample preparation is required, thus, the thin films were coated with carbon black.

Mechanical properties

Measurements of tensile mechanical properties of the prepared nanocomposites were performed on an Instron 3344 dynamometer, in accordance with ASTM D638, using a crosshead speed of 50 mm min^{-1}. Relative thin films of about 350.0 ± 25.0 μm thickness were prepared using an Otto Weber Type PW 30 hydraulic press connected with an Omron E5AX Temperature Controller, at a temperature of 140.0°C ± 5.0°C and a load of 50 kN on a ram of 100 mm. The molds were rapidly cooled by immersing them in ice water (∼ 0°C). From these films, dumb-bell-shaped tensile test specimens (central portions 5.0 × 0.5 mm^2 thick, 22.0 mm gauge length) were cut in a Wallace cutting press and conditioned at 25°C and 55–60% relative humidity for 48 h. The values of Young's modulus, yield stress, elongation at break and tensile strength at the break point were determined. At least five specimens were tested for each sample and the average values, together with their standard deviations, are reported.

Dynamic mechanical analysis (DMA)

The dynamic mechanical properties of the nanocomposites were measured with a Perkin–Elmer Diamond DMA. The bending (dual cantilever) method was used with a frequency of 1 Hz, a strain level of 0.04%, in the temperature range of −80.0–80.0°C. The heating rate was 3°C min^{-1}. Testing was performed using rectangular bars measuring ∼ 30 × 10 × 3.0 mm^3. These were prepared with a hydraulic press, at a temperature of 140°C under a load of 50 kN on a ram of 110 mm, for a time period of 5 min, followed by quenching in ice water (∼ 0°C). The exact dimensions of each sample were measured before the scan.

Rheology

Rheological characterization was carried out on a Reologica ViscoTech oscillatory rheometer using 20-mm parallel plate fixtures, with a gap of 0.5 mm at 120°C, under a nitrogen blanket. The rheometer was operated in the dynamic oscillatory mode in the linear viscoelasticity region. The elastic modulus (G'), loss modulus (G'') and complex viscosity (η^*) were measured as a function of angular frequency (ω).

Enzymatic hydrolysis

Samples in the form of films (10 × 20 × 0.4 mm^3, ∼100 mg) prepared using an Otto Weber Type PW 30 hydraulic press as described before, were placed in test tubes, wherein 5 mL of phosphate buffer solution (0.2*M*, pH 7.0) was added, containing *Pseudomonas cepacia* lipase. The concentration and catalytic activity of the lipase were 1.24 mg mL^{-1} and 0.176 U mL^{-1}, respectively. The loosely capped test tubes were kept at 50.0°C ± 1.0°C in an oven for several days while the media were replaced every 3 days. After a predetermined time the films were removed from the lipase solution, washed thoroughly with distilled water and ethanol and then dried at room temperature under vacuum, until constant weight. Every measurement was repeated three

times. As a control, the same experiment was carried out without lipase added under the same conditions. The degree of biodegradation was estimated from the mass loss. The morphology of the prepared films during enzymatic hydrolysis was examined using Scanning electron micrographs using a JEOL JMS-840 microscope. The operating conditions were: accelerating voltage 20 KV, probe current 45 nA and counting time 60 s. The samples were subjected to carbon black coating prior to the measurement.

RESULTS AND DISCUSSION

Nanocomposite preparation

PBSu/SiO_2 nanocomposites were prepared *in situ* during the synthesis of PBSu by the two-stage melt polycondensation method in the presence of fumed silica nanoparticles, as described in the Experimental section. At the first stage of esterification oligomers are formed, which have average molecular weights between 1500 and 2000 g mol^{-1}, while water is removed as by-product.[1] To prepare a material having high molecular weight, the polycondensation of these oligomers ensued at higher temperatures with the simultaneous application of high vacuum.

The number average molecular weight of PBSu that was prepared according to the described procedure was 57,000 g mol^{-1}, which is much higher than the molecular weight expected for typical aliphatic polyesters prepared by polycondensation. Similarly to previous reports on poly(ε-caprolactone),[30] the presence of SiO_2 nanoparticles in the polymerization mixture affected the reaction, leading to variations in the final molecular weights of the polymer. As shown in Figure 1, the number average molecular weight of nanocomposites fluctuated. Initially the molecular weight was increased for a SiO_2 concentration of 0.5 wt % and then gradually decreased for higher concentrations. However, in all nanocomposites, except in the case of the sample containing 5 wt % SiO_2, the measured molecular weights were higher compared to neat PBSu. In the latter sample an insoluble fraction (3.2 wt %) was observed. In all cases, especially with the addition of the SiO_2 nanoparticles, the measured molecular weights were particularly high for aliphatic polyesters prepared by polycondensation of the corresponding diol and dicarboxylic acid. Such molecular weights can typically be achieved only when the chain extenders are used in the polyesters.[31–33]

The surface silanol groups (≡Si—OH) of fumed silica nanoparticles have a slightly acidic nature. This renders them capable of reacting with alcohols, just like an acid.[34] The possibility of such a reaction between the surface silanol groups of fumed silica nanoparticles and the hydroxyl end groups of the

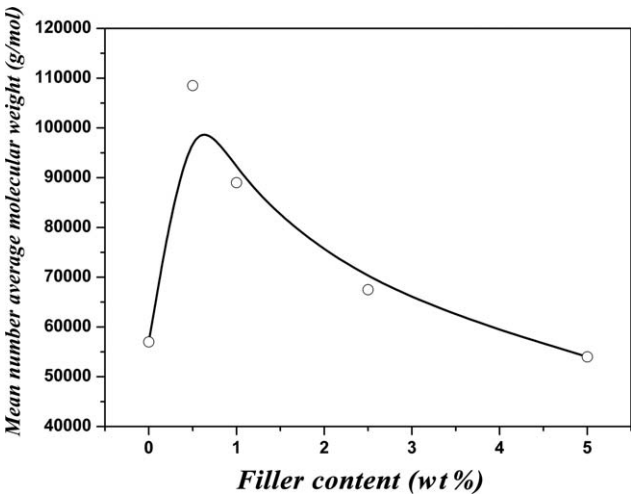

Figure 1 Variation of the number average molecular weight of the prepared materials as a function of the filler content, as measured by GPC.

polymer were first hinted in one of our previous study in nanocomposites consisted by poly(ethylene terephthalate) and fumed silica nanoparticles.[35] More substantiation was subsequently obtained by measurements from other authors using solid-state ^{29}Si NMR and FTIR on nanocomposites of fumed silica with PET[36,37] and PBSu,[23] indicating the possibility of covalent bonding between the fumed silica nanoparticles and the PBSu polymer backbone chain. In the present study ^{13}C NMR, was used to demonstrate the formation of a new bond. Given that the concentration of the filler in the samples was very low and, considering the slow kinetics of a silanol–alcohol reaction compared to a alcohol–carboxylic acid reaction, no new peak appeared in the ^{13}C NMR spectra. To bypass this problem an additional sample was prepared specifically for the study of the interaction between the additive and the polymer, having a particularly high concentration of fumed silica nanoparticles (25 wt %). During the polycondensation reaction the melt became extremely viscous, almost like a solid, which created stirring and heat transfer issues. Thus, the reaction could not be carried out for the desired time. Furthermore, the final material, in contrast to the other prepared materials, was completely insoluble in chloroform and other commonly used solvents in NMR. Such a decrease of solubility and behavior are usually observed in cases of covalent crosslinking of the pure polymer. To overcome this, the reaction was stopped at the esterification stage, with a simple application of vacuum for 15 min at the end to remove any unreacted monomers. In this way oligomers were obtained, having a number average molecular weight of 1500–2000 g mol^{-1}, which could perhaps be linear or branched, with a high concentration of SiO_2 nanoparticles and which, however,

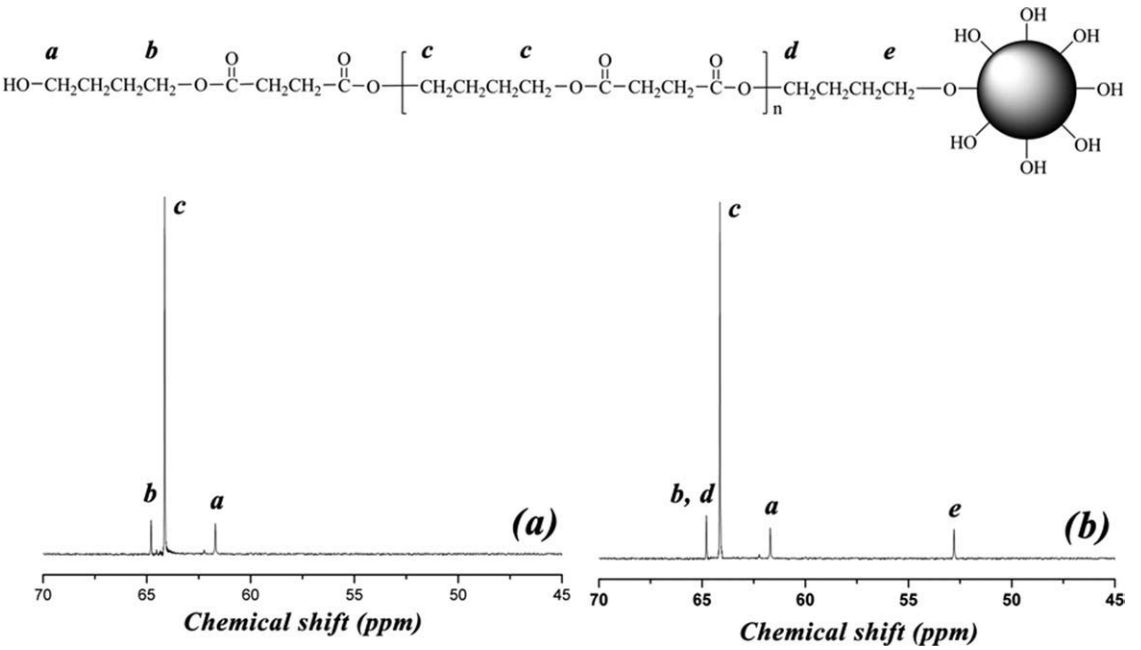

Figure 2 Proposed structure of PBSu hydroxyl end groups reacted with surface silanol groups of SiO_2, as well as ^{13}C NMR spectra of (a) pure PBSu and (b) its nanocomposite with SiO_2 (NMR sample).

were soluble in chloroform. The ^{13}C NMR spectra obtained for the pure polymer and the prepared oligomers containing a high concentration of fumed silica nanoparticles in the range of interest (70–45 ppm) are presented in Figure 2.

In the ^{13}C NMR of pure PBSu the methylene group next to the end hydroxyl group (a) gives a peak at 61.7 ppm, while the methylene group of the end butanediol next to the carbonyl group (b) gives a small peak at 64.8 ppm. The methylene group of butanediol next to the oxygen in the repeating unit of the oligomer (c) gives a strong peak at 64.1 ppm. The intensity of the peaks (a) and (b) is especially small in relation to (c), due to their small concentration in the oligomers.

In the oligomers prepared with fumed silica nanoparticles [Fig. 2(b)] a new peak (e) appeared at 52.8 ppm. This peak is attributed to the carbon involved in the bond C—O—Si, which is shifted to the right at higher field intensity. This is due to the electron back donation from oxygen to silicon via a (p→d orbital) π bond which causes the inactivity of the oxygen's lone electron pair, due to its overlapping with silicon's *d*-orbitals. Thus, less deprotection is expected of the carbon in comparison with the carbon which participates in the C—O—C bond and, consequently, shifting of the peak in areas of higher applied magnetic field, which is to the right of the spectra. Such a significant shift cannot be explained by the occurrence of hydrogen bonds between the hydroxyl end groups of the polymer and the surface silanol groups of SiO_2. Therefore, the formation of a covalent bond between the surface silanol groups of SiO_2 nanoparticles and the hydroxyl end groups of the polymer was confirmed by the aforementioned spectra in the prepared samples.

It seems that the silanol groups participate in the polymerization reaction just as carboxylic acids do, but at lower reaction rates compared to organic acids, due to their inorganic nature. Thus, the presence of the SiO_2 nanoparticles in the polymerization mixture, taking into account that this particular nanoparticles have a lot of surface silanol groups ($\sim$4.6 nm^{-2}) and specific surface area 200 m^2 g^{-1}, likely acts similarly to a multifunctional carboxylic acid. The polymer chains that are covalently bound onto the particle surface can act as bridges connecting the particles, thus leading to the formation of a branched and, as the polycondensation reaction proceeds, eventually to a crosslinked structure.

Taking into account the aforementioned findings an explanation for the variation of the molecular weights of the prepared nanocomposites can be proposed. The reaction of fumed silica as a coupling agent, together with the increased thermal conductivity of the polymerization mixture, due to the presence of the inorganic filler, led to an increase of the molecular weight.[38] However, at higher SiO_2 concentrations, due to the extended of the reactions between silanoil groups and hydroxyl end groups of PBSu, branched and even crosslinked macromolecules are formed (Fig. 3). It is well known that the hydrodynamic dimensions of branched polymers in solution are smaller compared to those of linear polymers with the same molecular weight.[39] Intrinsic viscosity and GPC measurements calculate the

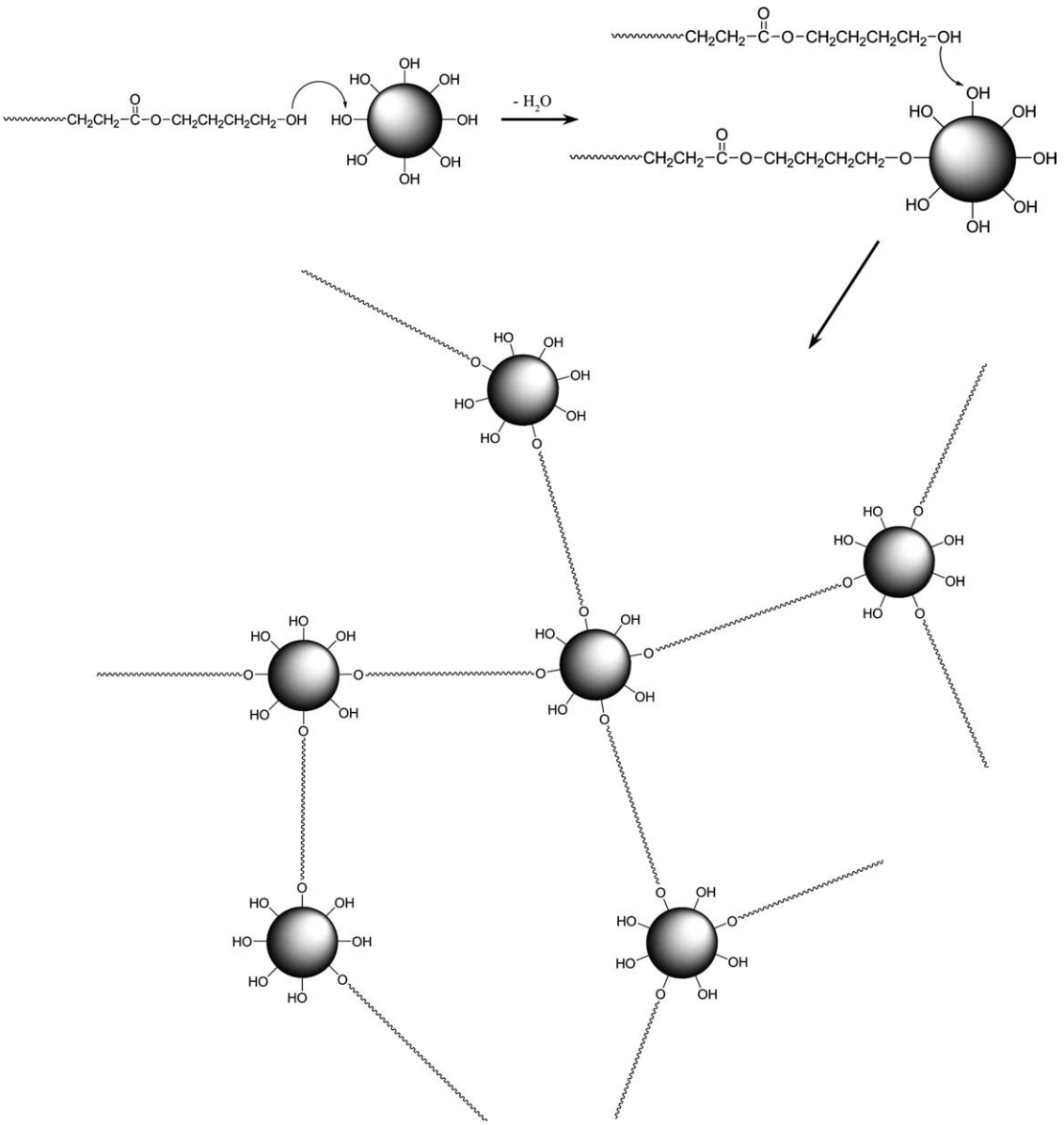

Figure 3 Reaction between the hydroxyl end groups of PBSu and the surface silanol groups of fumed silica nanoparticles, ultimately leading to the formation of a crosslinked polymer.

molecular weight of polymers based on their hydrodynamic size in solution. Therefore, branched polymers appear as having lower molecular weights in comparison to their actual one, and this may be the reason for the reduction in molecular weight seen in the samples containing concentrations of SiO_2 nanoparticles greater than 0.5 wt %.

Morphological characterization

Prior to the esterification reaction the fumed silica nanoparticles were dispersed in 1,4-butanediol, with the help of ultrasonic vibration and intense stirring, in an effort to optimize the dispersion of the particles. However, examining the prepared material with TEM (Fig. 4), it is clear that small aggregates and individual nanoparticles appear in the samples, coexisting with larger agglomerates. This is typical in cases when such nanoparticles are dispersed in nonpolar polymers, such as polyethylene and polypropylene.[40] However, large aggregates were reported in PBSu nanocomposites with SiO_2 and TiO_2,prepared by melt mixing,[23,41] where it was concluded that the sizes of the aggregates depended mainly by the nanoparticle content and screw rotation speed of the extruder during compounding. Such dependence was also observed in the present study with the sizes of the aggregates and agglomerates being directly related to the SiO_2 concentration. At the low concentrations of 0.5 and 1 wt % the filler exhibited better dispersion degrees with agglomerate sizes less than 100 nm. At the higher concentrations

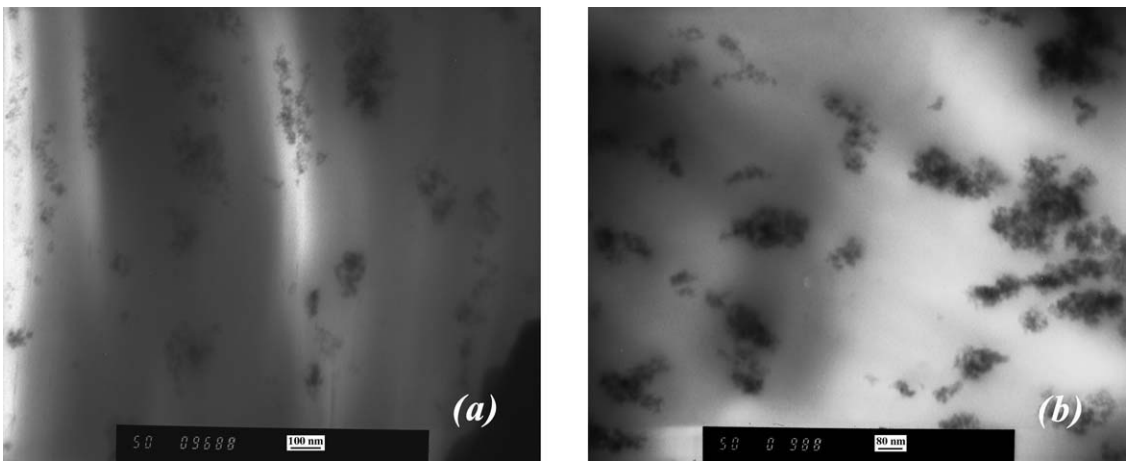

Figure 4 TEM micrographs of PBSu/SiO_2 nanocomposites containing (a) 2.5 wt % and (b) 5 wt % SiO_2.

of 2.5 and 5.0 wt % some larger agglomerates with maximum size of 200 nm were observed. These agglomerates are formed due to the relatively strong interactions between the surface silanol groups of fumed silica and it seems that the reactions between the PBSu macromolecules are not sufficient to ensure the complete dispersion of the filler in the form of individual nanoparticles.

Rheological properties

Further evidence of the structure of the composites was provided through rheological characterization. The curves for the storage moduli (G') and complex viscosities (η^*) of pure PBSu and its nanocomposites containing different amounts of nanoparticles are presented in Figure 5(a,b), respectively.

The sample containing 0.5 wt % exhibits a dramatic increase in G' and η^* over the entire frequency range. This is consistent with the increase in molecular weight noted in Figure 1. There is no evidence of branching in this sample, given that at low frequencies it approaches the terminal flow regime, where $G' \propto \omega^2$.

At filler loadings above 1 wt %, the response changes completely reflecting the changes in structure. Substantial deviations from terminal flow behavior are noted [Fig. 5(a)], accompanied by a loss of the Newtonian plateau, onset of yielding and pronounced shear thinning characteristics [Fig. 5(b)], resulting in high-frequency properties that are lower than the parent material. Such "pseudosolid"-like behavior is commonly observed in polymer matrices filled with nanofillers, and has been attributed to the formation of a filler–filler or polymer–filler percolated "network."[42] The theoretical percolation threshold for randomly dispersed spherical particles is about 30 vol %. However, it has been extensively shown that in nanosilica containing composites, the percolation threshold can be as low as 2 vol %,[43] which corresponds to about a 5 wt % loading.

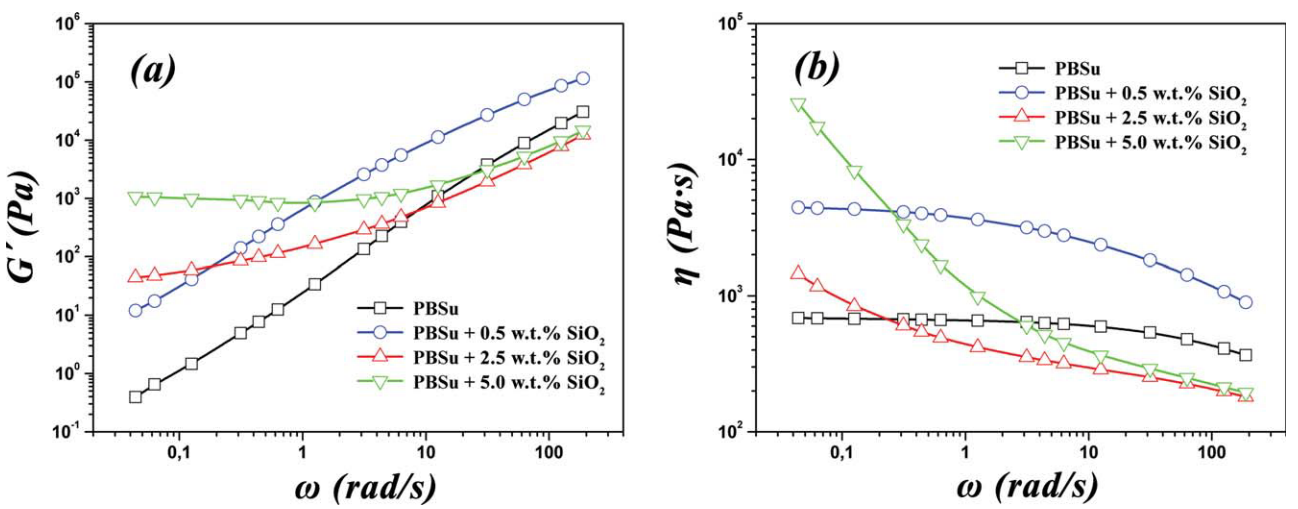

Figure 5 (a) Storage modulus (G') and (b) complex viscosity (η^*) as a function of silica content as a function of frequency at 120°C. [Color figure can be viewed in the online issue, which is available at wileyonlinelibrary.com.]

TABLE I
Thermal Analysis Results of the Prepared PBSu/SiO_2 Nanocomposites

Sample	T_m (°C)	T_c (°C)	ΔH_m (J g^{-1})	X_c (%)	ΔH_c (J g^{-1})
PBSu	116.7	84.4	109.3	52.0	92.6
PBSu + 0.5 wt % SiO_2	117.0	85.0	83.4	39.7	78.0
PBSu + 1.0 wt % SiO_2	116.8	86.9	77.6	37.0	74.0
PBSu + 2.5 wt % SiO_2	116.5	88.4	77.0	36.7	73.3
PBSu + 5.0 wt % SiO_2	116.3	90.6, 93.4	62.6	29.8	70.1

It is remarkable however that for the system under consideration in this work, pseudosolid like response appears at even lower loadings than this. Similar observations were recently made in PBSu nanocomposites with an organoclay.[14] They can be credited to the strong interactions of the fumed silica nanoparticles and the polymer matrix, resulting in the formation of covalent bonding, which leads to a highly branched structure. Furthermore, Zhang and Archer[43] reported that bridging of nanoparticles with adsorbed polymer molecules is substantially stronger for flocculated systems than for materials containing well-isolated nanoparticles. Two closely spaced nanoparticles can be easily bridged by adsorbed molecules, thus enhancing particle connectivity and reducing the mobility of the polymer chains. This appears to be the case for the system under consideration here, where the nanosilica particles are aggregated, as shown by the TEM images in Figure 4.

The presence of crosslinked gel in the sample containing 5 wt % silica further contributed toward the enhancement of the elastic modulus, to such an extent that it becomes independent of frequency in the low frequency range.

Thermal analysis

The DSC thermal analysis results of the prepared PBSu/SiO_2 nanocomposites are presented in Table I. The melting point of pure PBSu was 116.7°C. From the melting enthalpy, taking into account that the fully crystalline material has a heat of fusion of 210 J g^{-1},[44] it was calculated that the polymer had a degree of crystallinity equal to 52.0%. The melting point was not affected substantially upon addition of nanoparticles. The measured melting points are very close to each other. However, the degree of crystallinity was found to gradually decrease with increasing concentration of nanoparticles. For the nanocomposite containing 1 wt % nanoparticles the degree of crystallinity was calculated equal to 37%, while for the sample having 5 wt % of SiO_2 the degree of crystallinity was 29.8% (Table I). Even thought it was found that SiO_2 nanoparticles can increase the crystallization rate of a crystalline polymer[45] by acting as nucleating agents, they impart a negative effect upon the degree of crystallinity. Such behavior was also observed when using SiO_2 nanoparticles in HDPE, with the crystallization rates for the nanocomposites being higher compared to neat HDPE, whereas the degree of crystallinity was reduced.[46] Similar observations were reported for PBSu nanocomposites, whereas silica and silica-g-PBSu particles could act as nucleating agents during the crystallization process and accelerate the crystallization rates of the PBSu matrix.[24] Furthermore, with the addition of montmorillonite crystallinity was decreased, whereas the half-life of crystallization was increased.[47–49] The dispersed clay particles acted as a nucleating agent in the nanocomposites increasing the number of nuclei, causing the formation of smaller and irregular spherulites. Carbon nanotubes were also found to be able to play the role of a nucleating agent and enhance the crystallization rate of PBSu.[15] An additional reason for the dramatic decrease of the degree of crystallinity in the sample containing 5 wt % SiO_2 could be the presence of an extended branched and crosslinked structure, which constricts to a certain extent the motion of the macromolecular chains and lessens their freedom to move and be properly spatially arranged, as is prerequisite for the crystallization process.

The crystallization temperature of pure PBSu was at 84.4°C. With the addition of the nanoparticles a gradual shift to higher temperatures were observed, as the SiO_2 concentration increased. This is an indication that the nanoparticles acted as nucleating agents increasing the crystallization rate of PBSu, due to a heterogeneous nucleation process. More careful examination of the shape of the crystallization peaks revealed that the sample containing 5.0 wt % SiO_2 exhibited two crystallization peaks at 90.6 and 93.4°C, the second already having emerged as a shoulder at the sample containing 2.5 wt % SiO_2. This probably resulted because the nucleation activity of a particle depends on their size and, thus, in cases where significant size distribution of the dispersed phase exists, multiple peaks are recorded due to the different magnitude of the nucleation effect.

Tensile properties

The tensile properties of all samples are presented in Figure 6. The slightly reduced crystallinity of the nanocomposites due to the incorporation of the SiO_2 nanoparticles was expected to incur a negative effect. To exclude or at least diminish the effect of crystallinity on any observed mechanical properties' variation, the samples were quenched in ice water

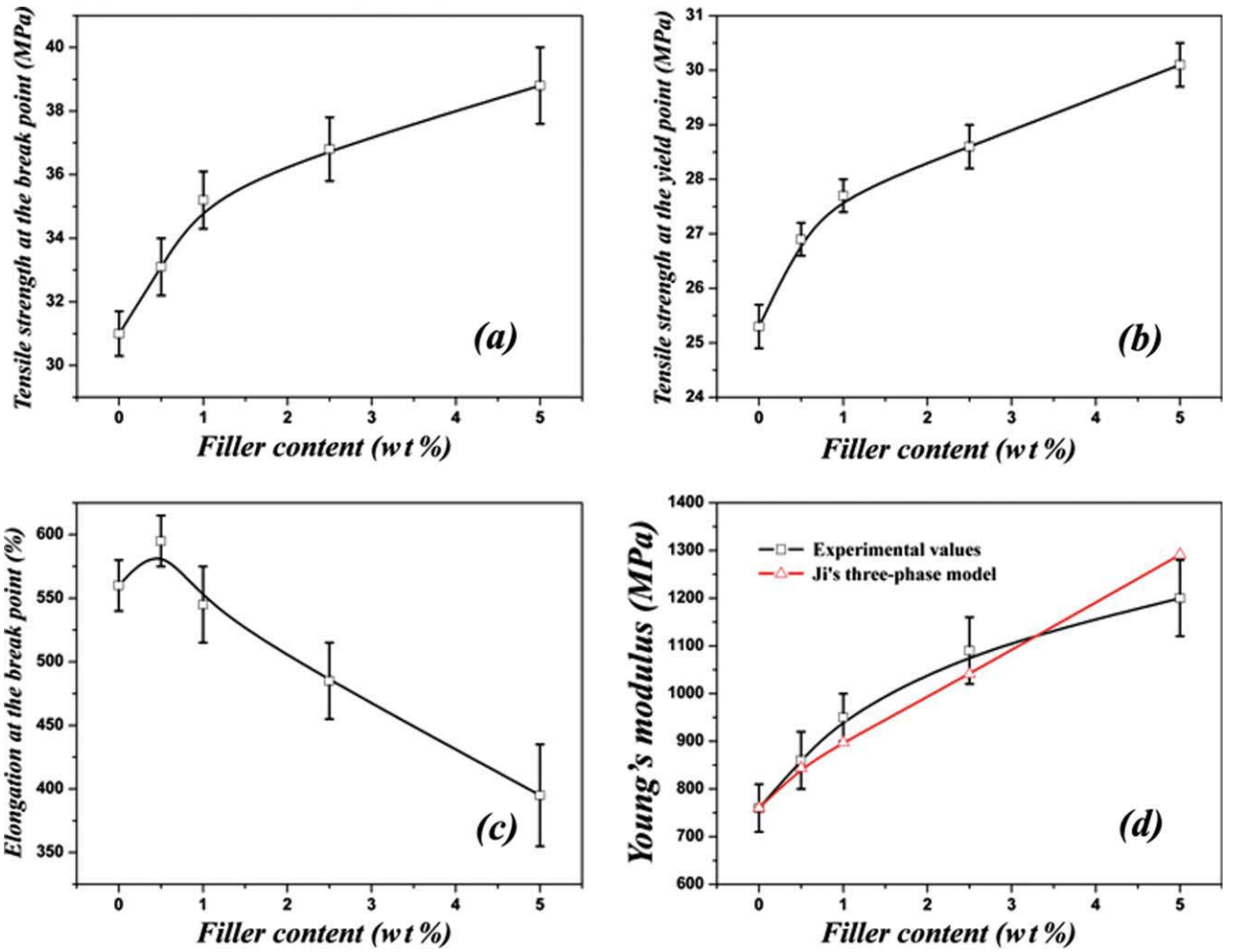

Figure 6 Mechanical properties of PBSu/SiO_2 nanocomposites versus SiO_2 content. (a) Tensile stress at yield, (b) Tensile stress at break, (c) elongation at break, and (d) Young's modulus. [Color figure can be viewed in the online issue, which is available at wileyonlinelibrary.com.]

from 140°C and, therefore, the degree of crystallinity of all samples should not change significantly. On the other hand, the presence of the nano-filler, as well as its reaction with the polymer matrix, were both expected to bring about a positive affect on the mechanical properties. Furthermore, excluding the sample containing 0.5 wt % SiO_2, the observed differentiation of the molecular weights wasn't expected to have a significant impact on the final mechanical properties of the material.[50] The substantial increase of molecular weight of the sample containing 0.5 wt % nanoparticles probably had a positive effect on the mechanical properties.

Comparing the results it is noticed that that tensile strength at yield point increased with increasing concentration of SiO_2, reaching a maximum increase of 19% for the nanocomposite containing 5 wt % SiO_2 [Fig. 6(a)]. This increase is an indication of adhesion between the polymer matrix and the inorganic nanoparticles. When the adhesion between the two phases is high, tensile strength at the yield point increases accordingly. A similar trend was also recorded for tensile strength at break with the addition of the fumed silica nanoparticles. The absence of large agglomerates, which could act as points of stress concentration and ultimate failure points of the material, probably contributed to this behavior. From our previous studies[51,52] it was deduced that mechanical properties deteriorated at higher nanoparticles' concentrations than 2.5 wt %, due to the formation of large agglomerates above this content. However, in the present study a maximum increase of tensile strength at the break point was recorded for the nanocomposite containing 5 wt %, which exhibited a maximum improvement equal to 25% [Fig. 6(b)]. Although, as mentioned above, this is rather unusual for such nanoparticles, from our previous study in chitosan/SiO_2 and poly(vinyl alcohol)/SiO_2 nanocomposites, due to the evolved interactions between the reactive groups of the polymers and the surface silanol groups of SiO_2, a continuous increase of mechanical properties was observed with increasing

silica concentration.[53] It is well known that branched and crosslinked macromolecules lead to a further increase of mechanical properties.[54] Elongation at break was negatively affected by the addition of nanoparticles. A gradual decrease was revealed that reached 29% for a concentration of 5 wt % SiO_2 [Fig. 6(c)]. The reduction of elongation at break is common because inorganic nanorarticles can't be extended, while for samples with higher SiO_2 content this reduction was probably due to the formed nanoparticles' agglomerates, as verified by TEM analysis. However some ductility was preserved, probably owing to the reaction of the nano-filler with the polymer matrix, which resulted in good interfacial adhesion.

Finally, the addition of the nanoparticles induced an increase of Young's modulus, which reached up to 58% for the sample containing 5 wt % SiO_2 compared to the corresponding value for the pure polymer [Fig. 6(d)]. This was not only the result of the effect of the presence of the rigid nanoparticles, finely dispersed in the polymer matrix, but also the formation of branched and crosslinked macromolecules, which are both known to increase the hardness and modulus of the final material.

A survey of the literature indicates that two-phase models are invalid in describing experimental results on mechanical properties of most polymer nanocomposites. When the volume fraction of the filler is the same, the smaller the particle size the higher its specific surface, leading to a shorter distance between neighboring particles. Considering the radius of gyration of most macromolecules, which is of the order of 10 nm, and the size of the nanoparticles used (12 nm), it is comprehensible that the macromolecules close to the surface of the solid surface will have different responses from those in the matrix, due to mechanical displacement from elongation or strain. Thus, a thin layer between the rigid dispersed phase and the matrix will have different mechanical responses both from the matrix and from the dispersed phase. Ji et al.[55] proposed a three-phase model based on Takayanagi's two-phase model, in which an interface region is introduced to interpret the tensile modulus enhancement of polymer nanocomposites as a function of dispersed phase volume fraction, matrix and interface, and in the case of spherical particles as the dispersed phase it takes the form of:

$$\frac{1}{E_c}=\frac{1-\sqrt{[(r+t)/r]^3\phi}}{E_m}+\frac{\sqrt{[(r+t)/r]^3\phi}-\sqrt{\phi}}{\{1-\sqrt{[(r+t)/r]^3\phi}\}E_m+\sqrt{[(r+t)/r]^3\phi}(k-1)E_m/\ln k}+\frac{\sqrt{V_d}}{\{1-\sqrt{[(r+t)/r]^3\phi}\}E_m+\{\sqrt{[(r+t)/r]^3\phi}-\sqrt{\phi}\}(k+1)E_m/2+\sqrt{\phi}E_f} \quad (1)$$

where k is a linear gradient change in modulus between the matrix and the surface of the particle ($1 < k < (E_d/E_m)$), r is the radii of the spherical particle and t the thickness of the interfacial region.

It becomes apparent [Fig. 6(d)] that using the three-phase model some correlation with the experimental results can be achieved. As predicted by the equation, as the size of the dispersed phase approaches the nanometer scale a dramatic increase in the modulus of the composite results. The deviation at higher filler loadings can be attributed to the formation of larger agglomerates, resulting in higher apparent filler particle sizes.

Dynamic mechanical analysis (DMA)

The temperature dependence of the storage modulus (E') and tan δ for all the prepared samples is presented in Figure 7. E' gradually decreases with increasing temperature and a transition is observed at about −30°C, which is ascribed to the glass transition temperature of the material (T_g). As the concentration of SiO_2 increases, so does the storage modulus of the material. Such a behavior was also mentioned in nanocomposites of PBSu with different ratios of organically modified layered silicates.[17] The extent of this reinforcement is limited below the T_g, probably because the PBSu matrix below this temperature, at which the molecular motion of the macromolecular chains themselves is largely restricted, may have a more substantial contribution to the modulus of each nanocomposite. However, above the T_g the incorporation of the nanoparticles significantly increases the storage modulus of the material, thus retaining the E' at a high level over a wide temperature range. The increase can be attributed to the restriction of the molecular motion of the PBSu macromolecules, due to the fine dispersion of the nanofillers, leading to increased interactions with the polymer matrix, as well as to the reaction between the two phases and the formation of a covalent bond, which further constrains the molecular motion

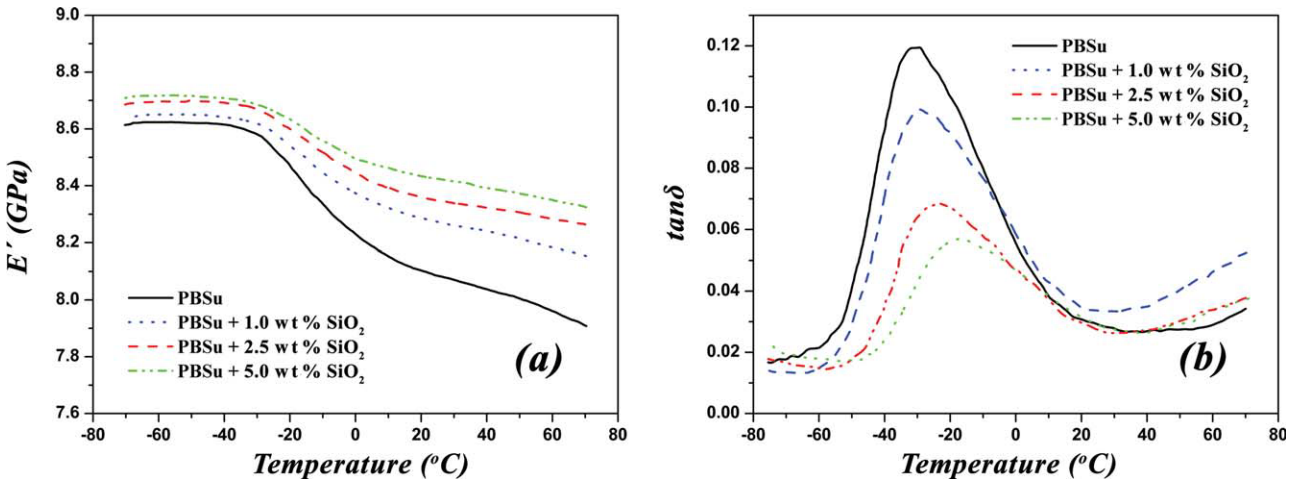

Figure 7 Variation of the storage modulus and tan δ of the prepared nanocomposites. [Color figure can be viewed in the online issue, which is available at wileyonlinelibrary.com.]

of the macromolecular chains. The effect of the decreased crystallinity didn't seem substantial enough to impart a visible negative influence on the storage modulus.

The tan δ curves revealed a large maximum around −30°C, which corresponded to the T_g of the prepared samples. For pure PBSu this value was found equal to −30.7°C. As the concentration of the incorporated nanoparticles increased so did the valued of the T_g. Specifically, it increased up to a maximum of −17.5°C for the sample containing 5.0 wt % fumed silica nanoparticles. Considering the radius of gyration of most macromolecules, which is of the order of 10 nm, it is conceivable that the motion of the macromolecules that are covalently bound to the surface of the solid surface is restricted, therefore leading to an increase in the T_g.[56] This lends further proof to the presence of covalent bonding between polymer and filler. Moreover, the presence of branching and/or crosslinking of the macromolecular chains may also contribute to the increase in the T_g value, since any motion of the macromolecular chains is hindered.

Finally, the value of tan δ at the T_g decreased with increasing the nanoparticles' concentration. This means that the dissipation energy at the T_g decreases as the nanofillers content increases, demonstrating that these materials may potentially have a structural damping property.

Degradability evaluation via enzymatic hydrolysis

Polyesters having a relative large number of methylene groups and those having α-ester and β-ester bonds with low T_m are hydrolysable by lipases.[1,12] A survey of the literature reveals that there is great confusion as far as the biodegradation of aliphatic polyesters is concerned. Almost all relevant studies deal with nanocomposites using layered silicates. In most cases an increase of the biodegradation rate was observed with the addition of the nanoparticles. It was concluded that the more hydrophilic the filler, the more pronounced the degradation.[57] This behavior was also explained by the presence of Al Lewis acid sites in the inorganic layers which catalyze the ester linkages hydrolysis. Furthermore, it was supported that intercalated layered silicates provide maximum part of the matrix being in contact with the clay edge and surface leading to a greater tendency to fragment more rapidly and hence ultimate degradation.

Enhanced biodegradation rates were also reported when using other nanoparticles with aliphatic polyesters. According to Han et al. the relative rate of biodegradation observed for PBSu/silica nanocomposites was faster than that of neat PBSu, indicating dependence on silica content.[23] The proposed explanation, similarly as in the case of layered silicates, was the increased hydrophilicity of the material due to the hydroxyl groups on the fumed silica's surface, which enhanced the susceptibility to microbial attack. Chouzouri and Xanthos found that the incorporation of calcium silicate or Bioglass 45S5 appeared to enhance the degradation behavior of both PCL and PLA.[58] Enhanced degradation behavior was attributed to the fact that the hydrophilic fillers enhanced the degree of swelling of the otherwise hydrophobic matrix.[59]

However, completely different findings on the effect of the nanoparticles on the biodegradation behavior have also been reported. Lee et al.[60] observed that the biodegradation rate of nanocomposites of aliphatic polyesters was decreased by the presence of layered silicates. They attributed this to the difficulty for the micro-organisms to reach the bulk matrix due to the barrier properties of the clay

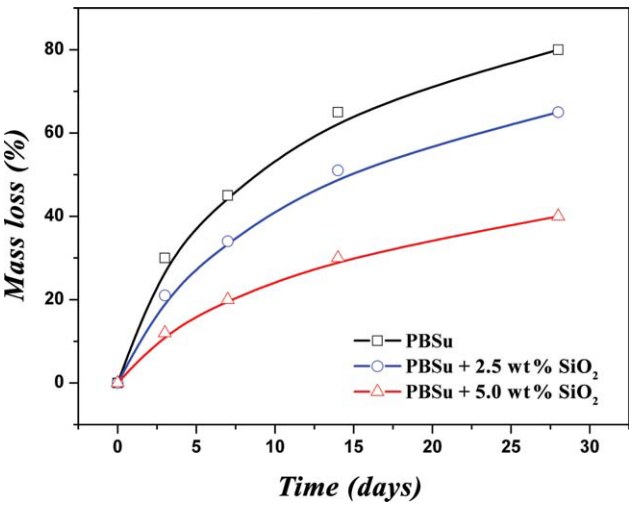

Figure 8 Mass loss of PBSu and its nanocomposites containing 2.5 and 5.0 wt % SiO_2 nanoparticles during enzymatic hydrolysis. [Color figure can be viewed in the online issue, which is available at wileyonlinelibrary.com.]

nanoparticles that make the diffusion path more tortuous. Very recently, Maiti et al.[61] also reported that the biodegradability of the poly(hydroxybutyrate) (PHB)/OMLS nanocomposites system was reduced after the addition of organically modified layered silicates. Such reductions of the biodegradation rate have been related to interactions of the matrix with the nano-filler, but also to water permeability, degree of crystallinity, and antimicrobial property of the nano-fillers studied.

In the present study the biodegradation rate was studied by enzymatic hydrolysis using a lipase. Lipases are endo-type enzymes degrading the ester bonds of macromolecular chains randomly and for this reason small variations in molecular weight don't affect the biodegradation rate. The weight loss of PBSu, as well as its nanocomposites with 2.5 and 5.0 wt % SiO_2, is shown in Figure 8. PBSu hydrolyzed up to 80 wt % after the lapse of 28 days. However, the sample containing 2.5 wt % of SiO_2 had only been hydrolyzed by 65 wt %, while the sample having 5.0 wt % SiO_2 by only 40 wt %. The hydrolysis rate of PBSu and its nanocomposites without lipase is very low and mass loss does not exceed 1.5 wt % after 28 days of hydrolysis. Furthermore, due to the low mass loss is not possible to find any clear difference between neat PBSu and its nanocomposites.

From the results it is clear that the addition of the nanoparticles reduced the enzymatic hydrolysis rate of PBSu, even though SiO_2, is a hydrophilic material,

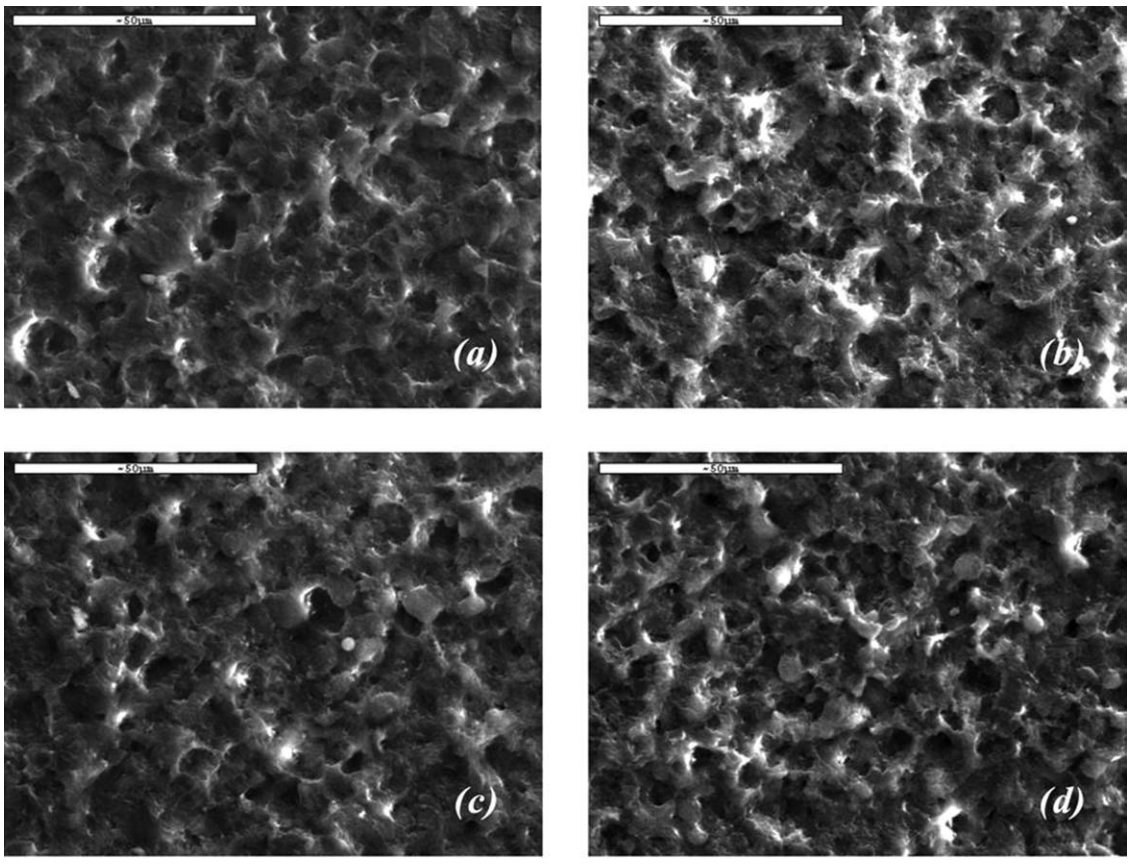

Figure 9 SEM micrographs of pure PBSu during enzymatic hydrolysis for (a) 3 days, (b) 7 days, (c) 14 days, and (d) 28 days.

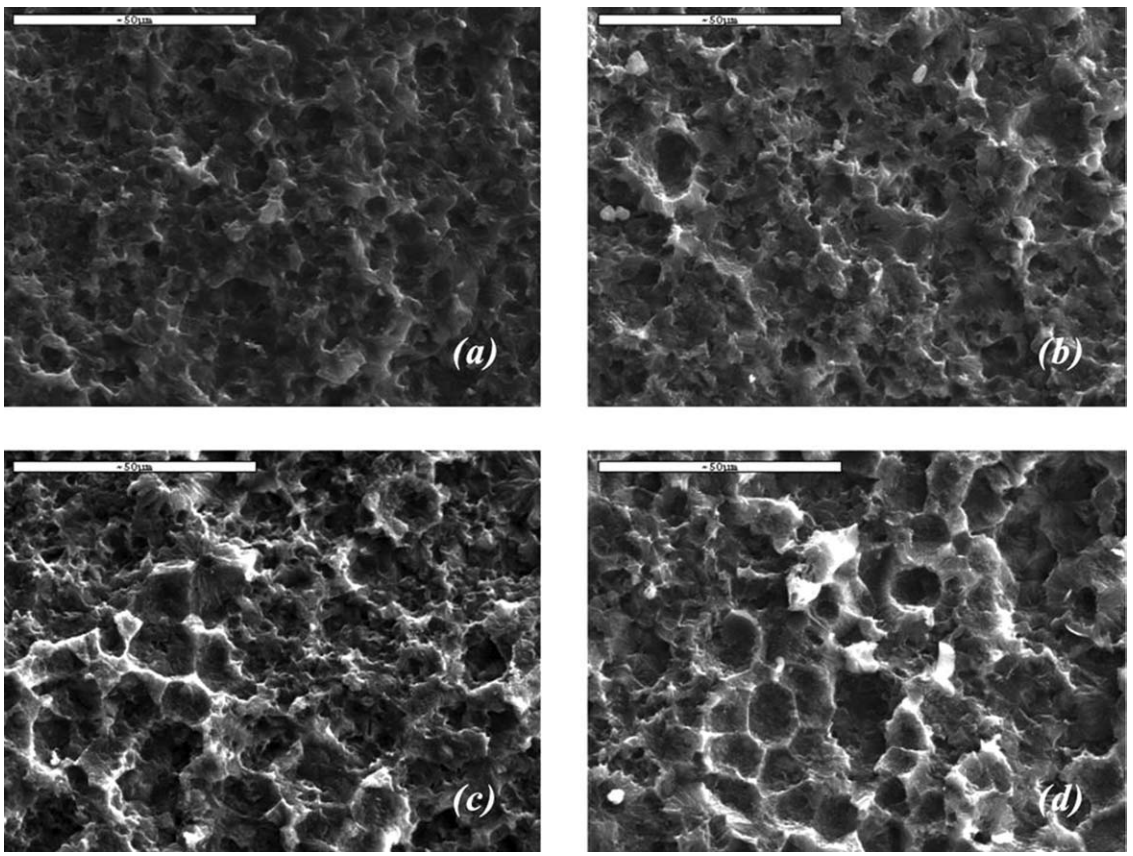

Figure 10 SEM micrographs of PBSu/SiO_2 nanocomposite containing 5 wt % SiO_2 nanoparticles during enzymatic hydrolysis for (a) 3 days, (b) 7 days, (c) 14 days, and (d) 28 days.

due to its surface silanol groups. Molecular weight, crystallinity, melting point, and available surface are important factors affecting the degradation characteristics of any biodegradable polymer. Usually, the lower the molecular weight and crystallinity, the faster the biodegradation. Semicrystalline polyesters, such as PBSu, degrade in two main stages. Initially, water diffuses into the amorphous regions, resulting in random hydrolytic scission of the ester groups, which may result in additional crystallization and an overall increase of crystallinity. After the initiation of the degradation of the major amorphous regions, hydrolytic attack shifts toward the center of the crystalline regions.

Taking the aforementioned into account, it would have been expected that the prepared nanocomposites, characterized by lower crystallinity and similar molecular weights to pure PBSu, should have been degraded faster compared to the pure polymer. However the opposite was observed. This reduction can be ascribed to mainly two different reasons. In the enzymatic hydrolysis of insoluble solid polymer, surface adsorption of the enzyme is the primary event of the reaction, the whole process being directly dependent on the available surface of the sample. The addition of inorganic nanoparticles, considering their extremely large surface area and fine dispersion, leads to the reduction of available surface for enzymatic hydrolysis. The inorganic nanoparticles can't be degraded by the lipase. A large portion of the outer surface of the polymer sample is replaced by the inorganic nanoparticles. Therefore, the surface available for enzymatic hydrolysis is significantly reduced and, thus, leads to reduced enzymatic hydrolysis rates and mass loss. The second possible cause of the observed behavior is the evolved interactions between the SiO_2 nanoparticles and PBSu, which lead to the formation of branched and crosslinked macromolecules. It is well known that these exhibit lower biodegradability rates compared to the corresponding linear ones. Overall, the biodegradability character of PBSu isn't hindered significantly by the incorporation of the nanoparticles.

Weight loss measurements provide a general trend of the enzymatic hydrolysis, but don't reveal how this hydrolysis proceeds. Thus, enzymatic hydrolysis was also studied by morphological examinations using SEM micrographs. As seen in Figures 9 and 10, even thought enzymatic hydrolysis is a heterogeneous process the whole surface of the samples had been eroded even at the first few days of enzymatic

hydrolysis. In the first few days the biodegradation of PBSu took place mainly in amorphous areas, revealing intact areas with crystallites (Fig. 9). Some holes appeared on the films' surface, which increased as the hydrolysis proceeded. The degradation progress of the prepared nanocomposites was also recorded (Fig. 10). However, even thought the enzymatic hydrolysis rate was lower in the nanocomposite containing 5 wt % SiO_2 nanoparticles, it was not possible to deduce such a decrease from the recorded micrographs. The evolution of the micrographs was similar to the corresponding ones of pure PBSu.

CONCLUSIONS

In PBSu/SiO_2 nanocomposites prepared by *in situ* polymerization, ^{13}C NMR spectra verified that the surface silanol groups of the SiO_2 nanoparticles had reacted with the hydroxyl end groups of the polymer, leading to the formation of covalent bonds. Because of these reactions the molecular weight of PBSu increased at low SiO_2 contents, while there was a gradual decrease at higher concentrations. SiO_2 nanoparticles acted as chain extenders at low contents, while at higher amounts the extended degree of reactions produced branched and crosslinked macromolecules. These subsequently resulted to a reduced degree of crystallinity, though the SiO_2 nanoparticles accelerated the crystallization rate of PBSu. These changes in structure were evident in the rheological characterization, wherein a pseudo-solid like response was observed during oscillatory shear measurements. The dynamic complex viscosity was increased as the concentration of SiO_2 also increased at low frequencies, leading to the formation of a yield stress.

Finely dispersed SiO_2 nanoparticles into the PBSu matrix were observed at low silica content, while some small agglomerates formed at higher concentrations. All tensile properties, except elongation at break, were significantly enhanced by the addition of the nanoparticles. Storage modulus (E') was increased, an increase more substantial at temperatures above the T_g of the polymer, which was, furthermore, gradually shifted to higher temperatures as the concentration of the nanoparticles increased.

Moreover, SiO_2 nanoparticles impacted a negative effect on the biodegradability of PBSu, since the enzymatic hydrolysis rate was reduced in the nanocomposites to about a half of the pure polymer's for the highest nanoparticles' concentration used. This was attributed to the smaller available surface area, due to the incorporation of the SiO_2 nanoparticles into the polymer matrix, and to the existence of branched and crosslinked macromolecules.

References

1. Bikiaris, D.; Papageorgiou, G.; Achilias, D. Polym Degrad Stab 2006, 91, 31.
2. Yasuniwa, M.; Satou, T. J Polym Sci Polym Phys 2002, 40, 2411.
3. Ihn, J. J.; Yoo, E. S.; Im, S. S. Macromolecules 1995, 28, 2460.
4. Ichikawa, Y.; Suzuki, J.; Washiyama, J.; Moteki, Y.; Noguchi, K.; Okuyama, K. Polymer 1994, 35, 3338.
5. Gan, Z.; Abe, H.; Kurokawa, H.; Doi, Y. Biomacromolecules 2001, 2, 605.
6. Qiu, Z.; Ikehara, T.; Nishi, T. Polymer 2003, 44, 2799.
7. Okada, M. Prog Polym Sci 2002, 27, 87.
8. Bhari, K.; Mitomo, H.; Enjoji, T.; Yoshii, F.; Makuuchi, K. Polym Degrad Stab 1998, 62, 551.
9. Doi, Y.; Kasuya, K.; Abe, H.; Koyama, N.; Ishiwatari, S.; Takagi, K.; Yoshida, Y. Polym Degrad Stab 1996, 51, 281.
10. Yoo, E. S.; Im, S. S. Macromolecules 1995, 28, 2460.
11. Uesaka, T.; Nakane, K.; Maeda, S.; Ogihara, T.; Ogata, N. Polymer 2000, 41, 8449.
12. Bordes, P.; Pollet, E.; Avérous, L. Prog Polym Sci 2009, 34, 125.
13. Shih, Y. F.; Wu, T. M. J Polym Res 2009, 16, 109.
14. Gcwabaza, T.; Ray, S. S.; Focke, W. W.; Maity, A. Eur Polym J 2009, 45, 353.
15. Shih, Y. F.; Chen, L. S.; Jeng, R. J. Polymer 2008, 49, 4602.
16. Makhatha, M. E.; Ray, S. S.; Hato, J.; Luyt, A. S. J Nanosci Nanotechn 2008, 8, 1679.
17. Shih, Y .F.; Wang, T. Y.; Jeng, R. J.; Wu, J. Y.; Teng, C. C. J Polym Environ 2007, 15, 151.
18. Ray, S. S.; Okamoto, K.; Okamoto, M. Macromolecules 2003, 36, 2355.
19. Someya, Y.; Nakazato, T.; Teramoto, N.; Shibata, M. J Appl Polym Sci 2004, 91, 1463.
20. Chen, G. X.; Kim, H. S.; Yoon, J. S. Polym Int 2007, 56, 1159.
21. Okamoto, K.; Ray, S. S.; Okamoto, M. J Polym Sci Polym Phys 2003, 41, 3160.
22. Chang, J. H.; Nam, S. W. Comp Interf 2006, 13, 131.
23. Han, S. I.; Lim, J. S.; Kim, D. K.; Kim, M. N.; Im, S. S. Polym Degrad Stab 2008, 93, 889.
24. Lim, J. S.; Hong, S. M.; Kim, D. K.; Im, S. S. J Appl Polym Sci 2008, 107, 3598.
25. Rhee, S. H.; Lee, Y. K.; Lim, B. S.; Yoo, J. J.; Kim, H. J. Biomacromolecules 2004, 5, 1575.
26. Miyata, N.; Fuke, K.; Chen, Q.; Kawashita, M.; Kokubo, T.; Nakamura, T. Biomaterials 2004, 25, 1.
27. Zou, H.; Wu, S.; Shen. J. Chem Rev 2008, 108, 3893.
28. Kim, J. W.; Kim, L. U.; Kim, C. K. Biomacromolecules 2007, 8, 215.
29. Vaia, R. A.; Maguire, J. F. Chem Mater 2007, 19, 2736.
30. Vassiliou, A. A.; Papageorgiou, G. Z.; Achilias, D. S.; Bikiaris, D. N. Macromol Chem Phys 2007, 208, 364.
31. Bikiaris, D. N.; Karayannidis, G. P. J Polym Sci Polym Chem 1995, 33, 1705.
32. Bikiaris, D. N.; Karayannidis, G. P. J Polym Sci Polym Chem 1996, 34, 1337.
33. Bikiaris, D. N.; Karayannidis G. P. J Appl Polym Sci 1996, 60, 55.
34. Bikiaris, D. N.; Vassiliou, A. A. In Nanocomposite Coatings and Nanocomposite Materials; Öchsner, A.; Ahmed, W.; Ali, N., Eds.; Trans Tech Publications: Switzerland, 2009; Chapter 4, pp. 129–194.
35. Bikiaris, D.; Karavelidis, V.; Karayannidis, G. Macromol Rapid Commun 2006, 27, 1199.
36. Wang, F.; Meng, X.; Xu, X.; Wen, B.; Qian, Z.; Gao, X.; Ding, Y.; Zhang, S.; Yang, M. Polym Degrad Stabil 2008, 93, 1397.
37. Yao, X.; Tian, X.; Xie, D.; Zhang, X.; Zheng, K.; Xu, J.; Zhang, G.; Cui, P. Polymer 2009, 50, 1251.
38. Achilias, D. S.; Bikiaris, D. N.; Karavelidis, V.; Karayannidis, G. P. Eur Polym J 2008, 44, 3096.

39. Zimm, B. H.; Kilb, R. W. J Polym Sci 1959, 37, 19.
40. Schaefer, D. W.; Justice, R. S. Macromolecules 2007, 40, 8501.
41. Miyauchi, M.; Li, Y.; Shimizu, H. Environ Sci Technol 2008, 42, 4551.
42. Cassagnau, P. Polymer 2008, 49, 2183.
43. Zhang, Q.; Archer, L. A. Langmuir 2002, 18, 10435.
44. Papageorgiou, G. Z.; Bikiaris, D. N. Polymer 2005, 46, 12081.
45. Papageorgiou, G. Z.; Achilias, D. S.; Bikiaris, D. N.; Karayannidis, G. P. Thermochim Acta 2005, 427, 117.
46. Chrissafis, K.; Paraskevopoulos, K. M.; Pavlidou, E.; Bikiaris, D. Thermochim Acta 2009, 485, 65.
47. Gopakumar, T. G.; Lee, J. A.; Kontopoulou, M.; Parent, J. S. Polymer 2002, 43, 5483.
48. Shih, Y. F.; Wang, T. Y.; Jeng, R. J.; Wu, J. Y.; Wuu, D. S. J Appl Polym Sci 2008, 110, 1068.
49. Chen, G. X.; Yoon, J. S. J Polym Sci Polym Phys 2005, 43, 817–826.
50. Grosvenor, M. P., Staniforth, J. N. Int J Pharm 1996, 135, 103.
51. Bikiaris, D. N.; Papageorgiou, G. Z.; Pavlidou, E.; Vouroutzis, N.; Palatzoglou, P.; Karayannidis, G. P. J Appl Polym Sci 2006, 100, 2684.
52. Bikiaris, D.; Vassiliou, A.; Pavlidou, E.; Karayannidis, P. Eur Polym J 2005, 41, 1965.
53. Chrissafis, K.; Paraskevopoulos, K. M.; Papageorgiou, G. Z.; Bikiaris, D. N. J Appl Polym Sci 2008, 110, 1739.
54. Bikiaris, D. N.; Karayannidis, G. P. Polym Int 2003, 52, 1230.
55. Ji, X. L.; Jing, J. K.; Jiang, W.; Jiang, B. Z. Polym Eng Sci 2002, 42, 983.
56. Wang, M. J. Rubber Chem Technol 1998, 71, 520.
57. Zhou, Q.; Xanthos, M. Polym Degrad Stab 2008, 93, 1450.
58. Chouzouri, G.; Xanthos, M. J Plast Film Sheet 2007, 23, 19.
59. Chouzouri, G.; Xanthos, M. Acta Biomater 2007, 3, 745.
60. Lee, S. R.; Park, H. M.; Lim, H.; Kang, T.; Li, X.; Cho, W. J. Polymer 2002, 43, 2495.
61. Maiti, P.; Batt, C. A.; Giannelis, E. P. Polym Mater Sci Eng 2003, 88, 58.